

# Differentially Private Image Classification by Learning Priors from Random Processes

Xinyu Tang\*, Ashwinee Panda\*, Vikash Sehwal, Prateek Mittal  
Princeton University

## Abstract

In privacy-preserving machine learning, differentially private stochastic gradient descent (DP-SGD) performs worse than SGD due to per-sample gradient clipping and noise addition. A recent focus in private learning research is improving the performance of DP-SGD on private data by incorporating priors that are learned on real-world public data. In this work, we explore how we can improve the privacy-utility tradeoff of DP-SGD by learning priors from images generated by random processes and transferring these priors to private data. We propose DP-RandP, a three-phase approach. We attain new state-of-the-art accuracy when training from scratch on CIFAR10, CIFAR100, and MedMNIST for a range of privacy budgets  $\epsilon \in [1, 8]$ . In particular, we improve the previous best reported accuracy on CIFAR10 from 60.6% to 72.3% for  $\epsilon = 1$ . Our code is available at <https://github.com/inspire-group/DP-RandP>.

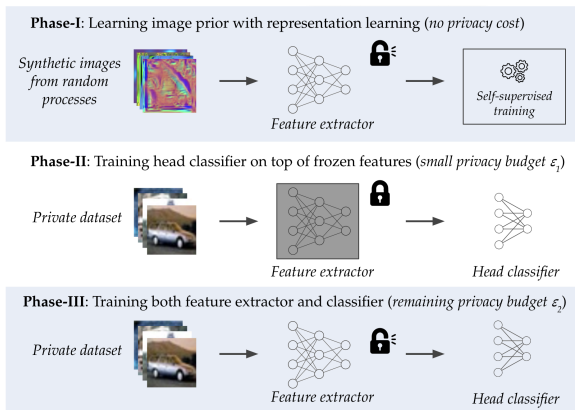


Figure 1: Our proposed DP training pipeline (DP-RandP) has three distinct phases. In Phase I, we sample images from random processes and train a feature extractor with representation learning to embed image priors beneficial for visual tasks. In Phase II, we spend a small privacy budget to train a linear classifier on top of extracted features of private data. In Phase III, we update all parameters with our remaining privacy budget. We demonstrate that incorporating image priors in Phase-I significantly improves DP training and adopting Phase II before training the whole network in Phase III can further improve test accuracy in DP training.

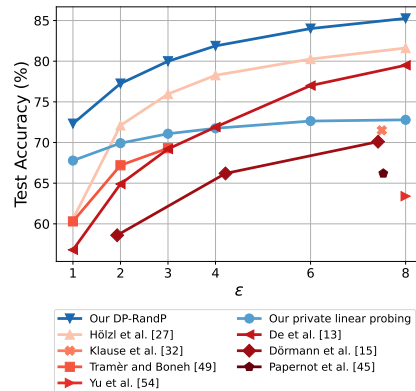


Figure 2: Comparing our results on CIFAR10 and previous state-of-the-art for  $(\epsilon, 10^{-5})$ -DP setup. Our full DP-RandP outperforms all previous works on this commonly benchmarked dataset and reduces the privacy cost needed to achieve 80% accuracy by a factor of  $e^3 \approx 20$  from  $\epsilon = 6$  to  $\epsilon = 3$ . Even our private linear probing from noise prior outperforms all previous work at  $\epsilon = 1$  but crucially has diminishing returns, a shortcoming that we address with our proposed three-phase DP training framework (DP-RandP).

\*Equal contribution. Correspondence to: Xinyu Tang <xinyut@princeton.edu>. Preprint, working version.

# 1 Introduction

Machine learning models are susceptible to a range of attacks that exploit data leakage from trained models for objectives such as training data reconstruction and membership inference [47; 3]. Differential Privacy (DP) is the gold standard for quantifying privacy risks and providing provable guarantees against attacks [17; 18]. DP implies that the outputs of an algorithm e.g., the final weights trained by stochastic gradient descent (SGD) do not change much (given by the privacy budget  $\epsilon$ ) across two neighboring datasets  $D$  and  $D'$  that differ in a single entry.

**Definition 1 (Differential Privacy)** *A randomized mechanism  $\mathcal{M}$  with domain  $\mathcal{D}$  and range  $\mathcal{R}$  preserves  $(\epsilon, \delta)$ -differential privacy iff for any two neighboring datasets  $D, D' \in \mathcal{D}$  and for any subset  $S \subseteq \mathcal{R}$  we have  $\Pr[\mathcal{M}(D) \in S] \leq e^\epsilon \Pr[\mathcal{M}(D') \in S] + \delta$ .*

Differentially Private Stochastic Gradient Descent (DP-SGD) [48; 1] is the standard privacy-preserving training algorithm for training neural networks on private data, with an update rule given by  $w^{(t+1)} = w^{(t)} - \frac{\eta_t}{|B|} (\sum_{i \in B} \frac{1}{c} \text{clip}_c(\nabla \ell(x_i, w^{(t)})) + \sigma \xi)$  where the changes to SGD are the per-sample gradient clipping  $\text{clip}_c(\nabla \ell(x_i, w^{(t)})) = \frac{c \times \nabla \ell(x_i, w^{(t)})}{\max(c, \|\nabla \ell(x_i, w^{(t)})\|_2)}$  and addition of noise sampled from a  $d$ -dimensional Gaussian distribution  $\xi \sim \mathcal{N}(0, 1)$  with standard deviation  $\sigma$ . DP-SGD introduces bias and variance into SGD and therefore degrades utility, creating a challenging privacy-utility tradeoff. For example, the state-of-the-art accuracy in private training is only 60.6% on CIFAR-10 at  $\epsilon = 1$  [27], while Dosovitskiy et al. [16] obtains 99.5% accuracy non-privately.

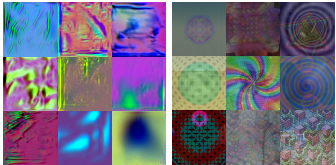
Theoretical analysis of the DP-SGD update yields that noise addition is especially harmful to convergence at the start of training [20], and that pretraining on public data can greatly improve convergence in this initial phase of optimization [38] by providing a better initialization [21]. Previous works have improved the privacy-utility tradeoff of DP-SGD by pre-training on large publicly available datasets, such as ImageNet [14], to learn visual priors [41; 40; 44; 8]. Other works assume that a small subset of in-distribution data is publicly available [53; 2; 37; 42].

Interestingly, previous work has uncovered that synthetic data learned from random processes [36; 9; 19; 30] can be used in representation learning [24; 11; 10] to learn highly useful visual priors [31; 4]. Because there is a large distribution shift between synthetic images and natural images, training on synthetic images does not incur any privacy cost. In this work, we leverage noise priors learned from synthetic images to boost the performance of DP training, and make the following key contributions:

- We find that while noise priors are only marginally helpful in non-private training, we can unlock their full potential to improve private training with a carefully calibrated training framework.
- We provide empirical evidence that priors learned from random processes become more critical as the privacy budget decreases, because priors provide fast convergence at the start of training, and have a much larger impact on private training than non-private training.
- We find that training a single linear layer (linear probing) on top of a pretrained feature extractor that has learned noise priors is more robust to large amounts of noise addition than end-to-end training of the entire network. We demonstrate this insight by linear probing with a small privacy budget  $\epsilon = 0.1$  to 57.1% on CIFAR10, achieving nontrivial performance with lower privacy cost than previous work has considered.
- We observe that while linear probing from noise prior has diminishing returns on performance as the privacy budget increases, end-to-end training of the entire network continues to improve with large  $\epsilon$  but critically struggles for small privacy budgets.
- We harness our insights by proposing a privacy allocation strategy that combines the benefits of learning from priors, linear probing, and full training into our full method DP-RandP (Visualized in Fig. 1). Our proposed approach pretrains a feature extractor on synthetic data to learn priors from random processes without paying privacy cost, then pays a small privacy cost for linear probing and makes the best use of our remaining privacy budget by updating all parameters to adapt our learned features to the private data.
- We evaluate DP-RandP against previous work and unlock new SOTA performance across CIFAR10, CIFAR100, and MedMNIST across all evaluated privacy budgets  $\epsilon \in [1, 8]$ . We provide a snapshot of our results in Fig. 2.

## 2 DP-RandP: Mitigating the Effects of Noise in DP-SGD with Noise Prior

We consider pretraining on synthetic data, generated by random processes [4; 5], as a *noise prior* in differentially private training. We consider synthetic images generated by random procedures, such as texture and fractal-like noise [5], or structure priors extracted from an untrained StyleGAN [4] (Figure 3). We use contrastive representation learning [11; 10; 24; 50], which aims to learn features invariant to common image transformations, to learn good visual features using synthetic images. At a high level, rather than using a random or ‘cold’ initialization for our downstream private dataset, we are using contrastive learning to obtain a ‘warm initialization’ that encodes priors learned from random processes. Across common natural vision tasks, noise priors also ensure that there is no privacy leakage from the pre-training data into this ‘warm initialization’.



(a) StyleGAN (b) Shaders  
 Figure 3: We use synthetic data generated from random processes in representation learning to learn useful image priors. Due to the high distribution shift from real images, we do not incur privacy costs when learning noise priors from these images.

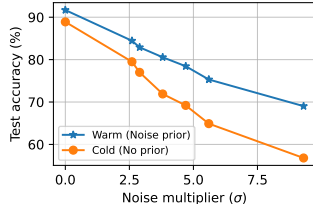


Figure 4: Comparison of training from a random initialization (cold) and pre-trained encoder on synthetic dataset (warm) across different privacy budgets (the x-axis is the corresponding  $\sigma$ ).

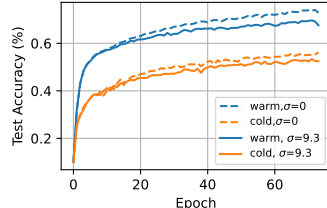


Figure 5: We zoom in on  $\sigma = 0, \sigma = 9.3$  with learning rate = 0.4 and find that the improvement of the warm start over cold start is mostly due to the initialization using synthetic dataset.

The fundamental question we seek to answer is how much noise prior benefits private training. As an initial exploration, we obtain a warm initialization via contrastive learning on synthetic images and compare it with a competitive DP-SGD baseline [13] that uses cold (random) initialization (Figure Fig. 4). We find that while the warm initialization only improves performance by 2.7% when  $\sigma = 0$ , i.e., non-private training, the warm initialization improves performance by 12.5% when  $\sigma = 9.3$  (equivalent to  $\epsilon = 1$ ). In Fig. 5, we zoom in on a single point of comparison between  $\sigma = 0$  (dashed) and  $\sigma = 9.3$  (solid) for warm and cold initializations. We find that over the course of training, as more noise is added, both the  $\sigma = 9.3$  warm and cold initializations not only converge at the same rate (given an appropriately small learning rate) but also diverge from the non-private runs at similar rates. *Although warm and cold start obtain different results in the private setting, the difference is mostly due to the initialization and is therefore magnified at smaller privacy budgets.*

We support this claim by drawing a connection to previous works. Ganesh et al. [21] prove the existence of out-of-distribution public datasets that can achieve small test loss on target private datasets. Bu et al. [7] prove that in the gradient flow setting for the NTK regime, that is, when we are taking very small steps  $\eta \rightarrow 0$ , noise does not impact convergence. Mehta et al. [41]; Panda et al. [44] propose scaling the learning rate  $\eta$  inversely with the noise  $\sigma$ . We combine our analysis with these previous works by noting that if we start training from fixed initialization and set the learning rate near-zero for small privacy budgets [41; 44], we enter the regime [7] where the noise does not impact convergence, and achieving nontrivial performance for these small privacy budgets provides the first empirical evidence for the theory [21] that *only the initialization matters*.

We gather our insights into a design goal that will enable us to achieve nontrivial performance under strict privacy constraints. We want to encode a learned prior into our initialization and then adapt this prior to private data. We now introduce DP-RandP, a method that achieves this key design goal.

### 2.1 Three-phase differentially private training framework

We propose a three-phase DP training framework DP-RandP that has two phases after pretraining on synthetic images, and significantly improves the performance of DP training (Figure 1). We first learn noise priors by training a feature extractor on synthetic data (Phase-I). We then split our private

training into 1) Learning the head classifier with frozen features (Phase-II) and 2) End-to-end training of the entire network to co-adapt the feature extractor and head classifier (Phase-III).

Our design is motivated by the strengths and weaknesses of linear probing and end-to-end training in the private setting. First, the  $\ell_2$  norm of the Gaussian noise added to gradients in each DP-SGD step scales with the number of parameters in the model. Because the head classifier typically has far fewer parameters than the feature extractor, updating this linear layer reduces the amount of added noise. Second, there is a large distribution shift between synthetic data from random processes and natural images found in private datasets. Linear probing merely inherits the frozen pre-trained features, but end-to-end training of all layers can improve the pre-trained features by adapting them to the private dataset. Because adapting to our private dataset may require many end-to-end training steps, we improve the convergence by first learning a task-specific linear classifier that can be trained quickly, and then training the entire network end-to-end. DP-RandP satisfies our previously stated design goal by first obtaining a good initialization with pretraining, then transferring the prior encoded in this initialization to the private dataset with fast-converging linear probing, and finally end-to-end training to adapt to the private dataset as much as possible for a given privacy budget.

We further consider the design choice of how to allocate the privacy budget for the two private training phases ( $\epsilon_1$  and  $\epsilon_2$ ). Recall that our model is pre-trained on synthetic data in Phase I, thus it doesn't incur any privacy cost. In Phase II, we use DP-SGD with privacy budget  $\epsilon_1$  to train the linear classifier. We observe diminishing returns in accuracy with increasing  $\epsilon_1$ , so we spend a smaller privacy budget on linear classifier training and allocate the rest to training the full network in Phase III. Allocating a higher budget to full training does not have diminishing returns; consider that  $\epsilon_2 = \infty$  we recover non-private accuracy. We now rigorously evaluate the performance of DP-RandP.

### 3 Evaluation

To outline the evaluation section we first overview our experimental setup and then evaluate the performance of DP-RandP in Sec. 3.2. We find that our method outperforms all previous works across multiple datasets, architectures, and privacy budgets. In Sec. 3.3 we find that our principled allocation of privacy budget  $\epsilon_1, \epsilon_2$  between linear probing and end-to-end training is robust to different choices of  $\epsilon_1$  and  $\epsilon_2$ . Finally we discuss the computational costs of our method and find that DP-RandP can provide computational savings over previous methods.

#### 3.1 Experimental setup

##### **Learning priors from images generated by random processes with representation learning.**

In Phase I we sample images from StyleGAN-oriented [4], and train a feature extractor on these synthetic datasets with representation learning [11; 50] with the loss function proposed in Wang and Isola [50]. Although our method can accommodate any kind of synthetic data and representation learning method, we focus our evaluation on these datasets and methods. We consider other kinds of synthetic data in Appendix A.

**Datasets and models.** We evaluate DP-RandP on CIFAR10/CIFAR100 [33], and DermaMNIST in MedMNIST [51; 52]. For CIFAR10/CIFAR100, we use WRN16-4 following De et al. [13]. For MedMNIST, we use ResNet-9 following Hölzl et al. [26]. We choose WRN16-4 and ResNet-9 because these architectures for the corresponding datasets achieve the most compelling results in previous works [13; 26]. We also report results of WRN40-4 on CIFAR10 in Appendix B.

**Implementation details.** To ensure a fair comparison with previous works [13; 46; 27], we use standard DP-SGD [1] and make use of multiple data augmentations and exponential moving average (EMA) as proposed by De et al. [13], that are now standard techniques used in DP-SGD work [46; 27]. We allocate small privacy budget  $\epsilon_1$  to Phase II and remaining privacy budget  $\epsilon_2$  to Phase III according to the strategy detailed in Sec. 3.3. We report our results across different privacy costs and use  $\delta = 10^{-5}$  for CIFAR10/CIFAR100/DermaMNIST by following previous works [13; 26].<sup>1</sup> When we report results, we report the standard deviation and accuracy averaged across 5 independent runs with different random seeds. We report all hyperparameters in Appendix C.

<sup>1</sup>We run experiments for  $\epsilon = \infty$  with per-sample gradient clipping but without noise, because we are interested in the ability of DP-RandP to mitigate variance. We note that there is accuracy degradation from the non-private baseline even at  $\epsilon = \infty$  due to the bias introduced by per-sample gradient clipping [29]. When we report  $\epsilon = \infty$  results from previous work we mark them with \* when previous work does not report whether the non-private baseline uses clipping.

### 3.2 Evaluation of DP-RandP

We report the results of DP-RandP in Tab. 1, Tab. 2 and Tab. 3 for CIFAR10, CIFAR100 and DermaMNIST datasets, respectively.

**DP-RandP outperforms all previous works across all privacy budgets.** In Table 1 we find that DP-RandP obtains higher performance than previous works [13; 27; 49; 32; 15; 54; 45] on CIFAR10 across the standard evaluated privacy budgets  $\epsilon \in [1, 8]$ .

We first compare DP-RandP to De et al. [13] as our CIFAR10 model, optimizer and hyperparameters follow De et al. [13]; the only difference is the use of Phase I and Phase II in DP-RandP to learn a prior from synthetic data and allocate a small privacy budget to linear probing. Crucially DP-RandP outperforms De et al. [13] by *more than 15%* for the important privacy budget  $\epsilon = 1$ .

Tramer and Boneh [49] use a ScatterNet [43] to encode invariant image priors and Hölzl et al. [27] use equivariant CNNs [12] to learn transform invariant features. DP-RandP shares the same intuition of leveraging invariant image priors as these two works [49; 27]. Instead of leveraging model architecture design for invariant features, we achieve this intuition by learning priors from images generated from random processes and design our three-phase framework to optimize use of this prior. Although DP-RandP shares this intuition of leveraging invariant image priors [49; 27], DP-RandP achieves 12% improvement over Tramer and Boneh [49]; Hölzl et al. [27] who both achieve 60% at  $\epsilon = 1$ . Our improvement comes both from leveraging the priors from synthetic images and our design of three learning phases that makes the best use of priors. We provide a detailed comparison to previous works [49; 27] in Sec. 4 where we explain why and how the feature prior we learn from synthetic data provides better results than the feature prior provided by their architectures.

Table 1: Test accuracy (%) of DP-RandP and comparison to previous work on CIFAR10. Not shown in this table are Klause et al. [32]; Dörmann et al. [15]; Papernot et al. [45]; Yu et al. [54] because they achieve 71.5% at  $\epsilon = 7.5$ , 70.1% at  $\epsilon = 7.42$ , 66.2% at  $\epsilon = 7.53$  and 63.4% at  $\epsilon = 8$  respectively, that are not on the pareto frontier of previous work. Note that Hölzl et al. [27] use a variant of WRN16-4 by leveraging an equivariant CNN.

Method	$\epsilon = 1$	$\epsilon = 2$	$\epsilon = 3$	$\epsilon = 4$	$\epsilon = 6$	$\epsilon = 8$	$\epsilon = \infty$
Tramer and Boneh [49]	60.3	67.2	69.3	–	–	–	71.1*
De et al. [13]	56.8	64.9	69.2	71.9	77.0	79.5	88.9
Hölzl et al. [27]	60.59	72.10	75.96	78.27	80.26	81.62	–
DP-RandP	72.32 <sub>0.22</sub>	77.25 <sub>0.07</sub>	79.99 <sub>0.21</sub>	81.88 <sub>0.27</sub>	84.01 <sub>0.23</sub>	85.26 <sub>0.11</sub>	91.69

**CIFAR100 results.** Previous work has not provided results on training from scratch for CIFAR100, perhaps because as we find in Table 2 the DP-SGD baseline following De et al. [13] does not perform well for  $\epsilon = 3$ . We believe this to be a competitive baseline, but DP-RandP outperforms it by more than 10% across  $\epsilon \in [3, 8]$ . Although CIFAR10 and CIFAR100 are both benchmark computer vision datasets, we find CIFAR100 to be a much more challenging task for private learning. One possible explanation for this is that private classifiers struggle to distinguish between many classes because the added noise is more likely to shift the decision boundary. We use the same hyperparameters for CIFAR10 and CIFAR100, that are likely suboptimal for CIFAR100, and the performance gap between  $\epsilon = 8$  and  $\epsilon = \infty$  may be mitigated if we train on CIFAR100 for longer than we do on CIFAR10. We encourage the use of CIFAR100 as a standard benchmark for private learning in the future because we find limited room for improvement on CIFAR10. In particular, the private and non-private gap between  $\epsilon = 8$  and  $\epsilon = \infty$  for CIFAR10 is only  $\approx 6\%$  for DP-RandP.

Table 2: Test accuracy (%) of DP-RandP and comparison to DP-SGD baseline on CIFAR100.

Method	$\epsilon = 3$	$\epsilon = 4$	$\epsilon = 6$	$\epsilon = 8$	$\epsilon = \infty$
DP-SGD	30.73	34.45	39.66	44.22	66.68
DP-RandP	43.33 <sub>0.15</sub>	46.40 <sub>0.31</sub>	51.53 <sub>0.13</sub>	55.02 <sub>0.21</sub>	71.68

**DermaMNIST results.** We have shown that DP-RandP outperforms previous work on the standard CV benchmarks of CIFAR10 and CIFAR100, and now consider the privacy sensitive medical dataset DermaMNIST. Although CIFAR is a standard CV benchmark, there is limited previous work that evaluates on privacy sensitive data in CV such as medical images. In Tab. 3 we find that DP-RandP achieve improvements from  $\epsilon = 1$  to  $\epsilon = 7.42$  by up to 2.78% over the DP-SGD baseline that we evaluate. Also, DP-RandP can achieve similar accuracy at  $\epsilon = 4$  as the result of DP-SGD at  $\epsilon = 7.42$ , which reduces the privacy cost as a factor of  $\epsilon^{3.42} \approx 30$ . We also include the results of Hölzl et al. [26], that use equivariant neural networks [12]. As we do not have access to the code of DP-SGD for equivariant CNN, we leave this as future work to investigate whether applying the equivariant neural network and our framework for learning from priors can further improve the utility as we provide a uniform framework DP-RandP, that is applicable to any model architectures.

Table 3: We follow previous work [26] and report the validation accuracy (%) of DP-RandP on DermaMNIST. We also report the test accuracy in Appendix D.

$\epsilon$	$\epsilon = 1$	$\epsilon = 4$	$\epsilon = 7.42$	$\epsilon = \infty$
baseline in Hölzl et al. [26]	—	—	72.41	78.48*
best in Hölzl et al. [26]	—	—	74.17	77.84*
DPSGD we evaluated	69.00 <sub>0.37</sub>	71.78 <sub>0.87</sub>	74.08 <sub>0.41</sub>	77.27
DP-RandP	71.78 <sub>0.40</sub>	74.82 <sub>0.55</sub>	75.91 <sub>0.29</sub>	79.26

We find that the prior we learn from synthetic data is applicable to standard benchmarks and medical images. One direction for future work is to validate the robustness of this prior across more datasets.

### 3.3 Allocating privacy budget in DP-RandP

In this subsection we analyze the privacy budgets of Phase II ( $\epsilon_1$ , linear probing) and Phase III ( $\epsilon_2$ , full training) and how to allocate the overall privacy budget  $\epsilon$  among Phase II and Phase III.

In Fig. 6 we observe that the performance of DP-RandP is robust to the key algorithmic design choice of how much privacy budget to allocate to Phase II and Phase III.

In particular, we find that even the worst choice of  $\epsilon_1/\epsilon$  provides results comparable to the previous SOTA on CIFAR10 at  $\epsilon = 1$ .<sup>2</sup> We first investigate the behavior at each extrema and conclude a general allocation strategy that provides good performance across CIFAR10, CIFAR100 and DermaMNIST.

**Allocating the entire privacy budget to Phase II is competitive for small privacy budgets but provides diminishing returns.** This corresponds to the right extreme in Fig 6 ( $\epsilon_1/\epsilon = 1$ ) and is equivalent to doing linear probing on top of extracted features. We follow the training recipe in Panda et al. [44] and report the result of private linear probing in Tab. 4 for CIFAR10 and Tab. 5 for ImageNet [14] respectively ( $\delta = 4 \times 10^{-7}$  for ImageNet, see Appendix E for experimental set-up).

We present the result of private linear probing on CIFAR10 by including more conservative privacy constraints like  $\epsilon = 0.03$ . Our private linear probing can achieve 57.10% at  $\epsilon = 0.1$ , that is comparable to the result of  $\epsilon = 1$  in De et al. [13] that fully trains a WRN16-4. Notably, previous work [49] also trains a linear classifier on top of the handcrafted features using an untrained ScatterNet [43]. DP-RandP is slightly better than their result at  $\epsilon = 3$ . We can see that our non-private baseline (74.05%) is slightly better than the non-private baseline (71.1%) in Tramer and Boneh [49], that

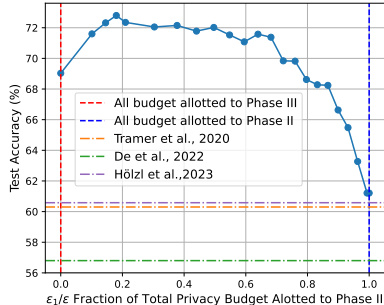


Figure 6: The fraction of total privacy budget allotted to Phase II for  $\epsilon = 1$ . The performance is stable across a wide range of value [0.1, 0.4]. However, skipping either Phase-II or Phase-III leads to suboptimal test accuracy in DP training.

<sup>2</sup>Due to computational constraints we were not able to calculate error bars for this ablation, resulting in some nonconvexity, but we will provide the updated figure with error bars in the next version.

Table 4: Test accuracy (%) of our private linear probing and comparison to previous private linear probing SOTA [49] on CIFAR10.

$\epsilon$	0.03	0.1	0.2	0.5	1	2	3
SOTA	-	-	-	-	60.3	67.2	69.3
Ours	40.64	57.10	60.89	65.10	67.78	69.92	71.08
(Std.)	2.59	0.42	0.26	0.21	0.17	0.09	0.14

Table 5: Test accuracy (%) of our private linear probing on ImageNet.

$\epsilon$	1	8
De et al. [13]	-	32.4
Sander et al. [46]	-	39.2
LP (RN50)	20.02	33.07
(Std.)	0.70	0.32

shows that our feature extractor is better than the ScatterNet and therefore improves the performance under DPSGD. We include a detailed comparison to Tramer and Boneh [49] in Sec. 4. However, this private linear probing variant of DP-RandP can only achieve 74.04% with no noise added, that is lower than the result at  $\epsilon = 4$  in De et al. [13], that shows that allocating all privacy cost to Phase II is a sub-optimal design choice.

We achieve comparable results on ImageNet to De et al. [13] using only linear probing on a ResNet50 pretrained from the Shaders21k dataset [5]. However, the state-of-the-art [46] performs extensive hyperparameter, architecture, and data augmentation search and obtains better performance than DP-RandP for  $\epsilon = 8$ . We lack the computational resources to perform full training at the scale of Sander et al. [46] who used 32 A100 GPUs. However, we note that we can achieve half the accuracy of Sander et al. [46] with  $\epsilon = 1$  even with private linear probing only, and aim to update the next version of this work with full results on ImageNet.

**Allocating the entire privacy budget to Phase III struggles for small privacy budgets.** We report DP-RandP without Phase II on CIFAR10 in Tab. 6 (equals to  $\epsilon_1/\epsilon = 0$  in Fig. 6). The result in Tab. 6 is slightly worse than DP-RandP in Tab. 1 and the utility gap between Tab. 6 and Tab. 1 decreases as  $\epsilon$  increases, that justifies the importance of Phase II in DP-RandP. Moreover, the result of DP-RandP without Phase II is significantly better than previous SOTA [13; 27; 49], that shows that the feature extractor pretrained on images from random process can capture the image prior.

Table 6: Fully privately training a WRN16-4 from the pretrained WRN feature extractor.

$\epsilon = 1$	$\epsilon = 2$	$\epsilon = 3$	$\epsilon = 4$	$\epsilon = 6$	$\epsilon = 8$	$\epsilon = \infty$
69.03 <sub>0.23</sub>	75.31 <sub>0.28</sub>	78.44 <sub>0.19</sub>	80.56 <sub>0.12</sub>	82.90 <sub>0.10</sub>	84.45 <sub>0.09</sub>	91.69

**A general privacy budget allocation strategy.** We have observed that allocating the entire privacy budget to linear probing or full training is suboptimal. We now propose a simple yet effective general strategy to allocate the privacy budget. For small  $\epsilon$  ( $\epsilon \ll 1$ ), we set  $\epsilon_1 = \epsilon$  to allocate the entire privacy budget to Phase II. This is because allocating the entire privacy budget to linear probing is competitive for small privacy budgets. As  $\epsilon$  increases, we decrease  $\epsilon_1/\epsilon$ . This is because as  $\epsilon$  increases, the noise multiplier will decrease. Therefore, it is easier to train the linear probing layer as  $\epsilon$  increases, and the percentage of total steps allocated to Phase II can be reduced to train a good linear probing layer and we can use the remaining steps for Phase III. Because the closed-form computation of  $\epsilon$  with PRV accounting [22] is challenging, we implement this strategy by using a fixed number of steps  $n$  for linear probing in CIFAR10, CIFAR100, DermaMNIST, and increasing the number of steps in Phase III as  $\epsilon$  increases. We present the privacy allocation  $\epsilon_1/\epsilon$  on CIFAR10 in Appendix F for results in Table 1, which validates this strategy.

### 3.4 Computational cost

DP-RandP consists of three phases. Some phases can be done in a single-run per dataset. For example, for feature extractor in Phase I, we only need to train a single feature extractor once for each evaluated dataset as the synthetic dataset and model architectures are the same. Also, for the private linear probing (LP). We report the computation cost in Tab. 7 for single-run per dataset. For Phase II and Phase III, we need to go through these processes at each run of our training process. Also, after we

Table 7: One-time per dataset computational cost on CIFAR10. These procedures only need to be done once for each evaluated dataset. Phase I can be shared for CIFAR10 /CIFAR100.

	Phase I	feature extraction in LP
Time	16 h	1 min

Table 8: Computational cost on CIFAR10 for hyper-parameters given in Appendix C. These procedures are comparable to the standard training procedure such as De et al. [13].

	linear probing in LP	Phase II	Phase III
Time	1 min	12min	5.5 h

get the extracted features for LP, we need to train a linear layer each time we run the experiments. We report the computation cost in Tab. 8 for these procedures.

De et al. [13] also needs to fully train a WRN16-4 and the major additional computation cost for DP-RandP is Phase I compared to De et al. [13]. However, the training in Phase I is done once for CIFAR10. Moreover, we can use the same feature extractor from Phase I for CIFAR10 and CIFAR100.

For the private linear probing experiment, each run of training a linear layer can be finished in 1 minute for CIFAR10 and 180 minutes for ImageNet while fully privately training a model costs much more time. A single run to privately train a WRN16-4 for CIFAR10 takes around 5.5 hours for 875 steps with 1 A100 GPU in our evaluation. Also, as reported in previous work [46], a single run for ImageNet experiments needs to take four days using 32 A100 GPUs.

## 4 Discussion and Related Work

In this section we provide a detailed comparison to two previous works [49; 27] that also use priors to improve DP-SGD image classification, and an overview of the broader body of work on improving the privacy utility tradeoffs in DP-SGD.

We provide a detailed comparison to the previous work of Tramer and Boneh [49], who find that linear probing on top of ‘handcrafted’ ScatterNet [43] features outperforms private ‘deep’ learning. While this linear probing performs well for smaller values of  $\epsilon$ , the non-private accuracy is limited because the features cannot be adapted to the private data. There are two key differences between DP-RandP and Tramer and Boneh [49]; we have much more flexibility in learning priors, and we have a more refined method for transferring features learned without privacy cost to private data. In Phase I we use representation learning to train the feature extractor on images sampled from random processes, in order to learn the prior to extract features that are invariant to transformations. Our feature extraction process is therefore much more general, and while we explore the use of different types of synthetic data, different model architectures, and different representation learning method, there are many more methods in each of these categories that we have not explored. The second difference is between linear probing, that is used by Tramer and Boneh [49] and that we consider as a baseline in Fig. 2, and the combination of linear probing and full training that we use in DP-RandP. Comparing the improvements between DP-RandP and Tramer and Boneh [49] confirms that our empirical improvements are mostly due to the advantage of DP-RandP over DP linear probing. In particular, for  $\epsilon = 3$ , exchanging the handcrafted features of Tramer and Boneh [49] for the pretrained feature extractor we use only improves performance by a modest  $\sim 2\%$ . However, our full DP-RandP exhibits a  $> 10\%$  improvement. Our innovation over Tramer and Boneh [49] is therefore twofold: we introduce the potential of pretraining on synthetic data for the DP community, and also provide guidance on how to better transfer features learned from synthetic data to private training.

Recently [26; 27] propose the use of inductive bias via architectural prior. They use DP-SGD to train the equivariant CNN architecture [12], and report results on the MedMNIST and CIFAR10, but have not provided code to reproduce their results. We note that the design space of novel architectures that are especially compatible with DP is rich and mostly unexplored, and our approach is compatible with any advancements in this domain. In particular, we could use the architecture of Hölzl et al. [26, 27] in our method and potentially enjoy the improvements of their method stacked on top of our own improvements by combining the feature priors. Because we lack the ability to implement the necessary per-sample gradient computation for equivariant CNNs, we instead compare our method using a standard ResNet to their results. We look forward to investigating whether applying the equivariant neural network and our framework for learning from priors can further improve the utility once the authors release their code.

**DP with public data** A major direction in improving the privacy utility tradeoff in DP-SGD is the principled use of public data. The most common method is to pretrain a feature extractor on public datasets such as ImageNet and then transfer the learned features to the private dataset. Our work is complementary to these techniques; we use the methods in Panda et al. [44] for Phase II of DP-RandP, and we believe that our use of linear probing and subsequent full training can also be applied to fine-tuning pretrained models from real-world images. However, we consider a different threat model to this line of work where we do not have access to public data and must instead make the best possible use of images drawn from random processes.

Several works [53; 2; 37; 42] make use of public data under a different threat model by treating a small fraction of the private training dataset as public. They find that, a small fraction of public data, e.g., 2000 public data on CIFAR10, can improve performance significantly on the DP-SGD baseline. The most recent work in this line [42] can achieve 72.1% on CIFAR10 at  $\epsilon = 1$  using the WRN16-4. Our result on CIFAR10 at  $\epsilon = 1$  using the same architecture (72.3%) is comparable to Nasr et al. [42]. This indicates that the prior learned from images generated from random processes can help as much as the prior learned from limited in-distribution public data.

Another line of work has shown the success of DP-SGD fine-tuning of pretrained large language models (LLMs) [23; 39; 55]. LLM pretraining can be framed as a way to learn structural priors from unstructured data [6].

**DP-SGD training from scratch** In addition to the directly related works discussed above, the baselines for training from scratch that we compare to in this work are De et al. [13] and Sander et al. [46]. De et al. [13] make use of multiple techniques that are now a mainstay of DP-SGD training from scratch such as multiple data augmentations [25] that we also use. Sander et al. [46] propose a method for estimating the best hyperparameters for DP training at scale using smaller-scale runs. Sander et al. [46] use 32 A100 GPUs for a month to train a single model on ImageNet, but we are unable to do an exact comparison because we lack their computational resources.

**Synthetic data for pretraining the model** Pretraining the model [16] on a large dataset like ImageNet and then adapting to domain-specific tasks [35] can help the model performance and convergence rate. Recent progress in computer vision has shown that it is possible to pretrain models with synthetic images from random processes without real-images [4; 5; 31] to learn the visual priors.

## 5 Limitations

**Assumptions.** The key assumption in learning priors from images generated by random processes without paying privacy cost is that there is no privacy leakage from the synthetic data to the private datasets that we consider. This assumption is shared with many recent works that study improving the performance of DP-SGD with pretrained models [41; 40; 8; 44; 42]. In contrast to these prior works that treat ImageNet as public data or a limited set of images from CIFAR as public, we treat the random process that generates our synthetic dataset as public. We inherit this assumption from the works that propose these synthetic datasets [4; 5].

**Scope of Claims.** We only evaluate datasets where we can compare the performance of DP-RandP to previous work that improves the performance of DP-SGD. We only evaluate using architectures that previous work has used. We only provide error bars across 5 runs with different random seeds.

**Key Factors that Influence the Performance of Our Approach.** The key factor in the performance of DP-RandP is the choice of total privacy budget  $\epsilon$  to allocate to Phase II and Phase III. In Sec. 3.3 we provide comprehensive analysis for our principled choice of privacy allocation, and also find that the performance of DP-RandP is robust to any allocation strategy in Fig. 6.

## 6 Conclusion

We leverage images generated from random processes and propose a three-phase training DP-RandP to optimize the use of noise prior. The evaluation across multiple datasets show that DP-RandP can improve the performance of DP-SGD. For example, DP-RandP improves the previous best reported accuracy on CIFAR10 from 60.6% to 72.3% at  $\epsilon = 1$ . DP-RandP is a general framework for different datasets, model, and representation learning methods and can be further investigated in future work.

## Acknowledgements

This work was supported in part by the National Science Foundation under grant CNS-2131938, the ARL’s Army Artificial Intelligence Innovation Institute (A2I2), Schmidt DataX award, and Princeton E-affiliates Award.

## References

- [1] M. Abadi, A. Chu, I. Goodfellow, H. B. McMahan, I. Mironov, K. Talwar, and L. Zhang. Deep learning with differential privacy. In *Proceedings of the 2016 ACM SIGSAC Conference on Computer and Communications Security*, pages 308–318. ACM, 2016.
- [2] E. Amid, A. Ganesh, R. Mathews, S. Ramaswamy, S. Song, T. Steinke, T. Steinke, V. M. Suriyakumar, O. Thakkar, and A. Thakurta. Public data-assisted mirror descent for private model training. In *Proceedings of the 39th International Conference on Machine Learning*, pages 517–535. PMLR, 2022.
- [3] B. Balle, G. Cherubin, and J. Hayes. Reconstructing training data with informed adversaries. In *2022 IEEE Symposium on Security and Privacy (SP)*, pages 1138–1156. IEEE, 2022.
- [4] M. Baradad, J. Wulff, T. Wang, P. Isola, and A. Torralba. Learning to see by looking at noise. In *Advances in Neural Information Processing Systems*, 2021.
- [5] M. Baradad, R. Chen, J. Wulff, T. Wang, R. Feris, A. Torralba, and P. Isola. Procedural image programs for representation learning. *Advances in Neural Information Processing Systems*, 35: 6450–6462, 2022.
- [6] T. Brown, B. Mann, N. Ryder, M. Subbiah, J. D. Kaplan, P. Dhariwal, A. Neelakantan, P. Shyam, G. Sastry, A. Askell, S. Agarwal, A. Herbert-Voss, G. Krueger, T. Henighan, R. Child, A. Ramesh, D. Ziegler, J. Wu, C. Winter, C. Hesse, M. Chen, E. Sigler, M. Litwin, S. Gray, B. Chess, J. Clark, C. Berner, S. McCandlish, A. Radford, I. Sutskever, and D. Amodei. Language models are few-shot learners. In H. Larochelle, M. Ranzato, R. Hadsell, M. Balcan, and H. Lin, editors, *Advances in Neural Information Processing Systems*, volume 33, pages 1877–1901. Curran Associates, Inc., 2020. URL [https://proceedings.neurips.cc/paper\\_files/paper/2020/file/1457c0d6bfc4967418bfb8ac142f64a-Paper.pdf](https://proceedings.neurips.cc/paper_files/paper/2020/file/1457c0d6bfc4967418bfb8ac142f64a-Paper.pdf).
- [7] Z. Bu, H. Wang, and Q. Long. On the convergence and calibration of deep learning with differential privacy, 2022.
- [8] Z. Bu, Y.-X. Wang, S. Zha, and G. Karypis. Differentially private optimization on large model at small cost, 2022.
- [9] G. J. Burton and I. R. Moorhead. Color and spatial structure in natural scenes. *Applied optics*, 26(1):157–170, 1987.
- [10] T. Chen, S. Kornblith, M. Norouzi, and G. Hinton. A simple framework for contrastive learning of visual representations, 2020.
- [11] X. Chen, H. Fan, R. Girshick, and K. He. Improved baselines with momentum contrastive learning. *arXiv preprint arXiv:2003.04297*, 2020.
- [12] T. Cohen, M. Weiler, B. Kicanaoglu, and M. Welling. Gauge equivariant convolutional networks and the icosahedral CNN. In K. Chaudhuri and R. Salakhutdinov, editors, *Proceedings of the 36th International Conference on Machine Learning*, volume 97 of *Proceedings of Machine Learning Research*, pages 1321–1330. PMLR, 09–15 Jun 2019. URL <https://proceedings.mlr.press/v97/cohen19d.html>.
- [13] S. De, L. Berrada, J. Hayes, S. L. Smith, and B. Balle. Unlocking high-accuracy differentially private image classification through scale. *arXiv preprint arXiv:2204.13650*, 2022.
- [14] J. Deng, W. Dong, R. Socher, L.-J. Li, K. Li, and L. Fei-Fei. Imagenet: A large-scale hierarchical image database. In *2009 IEEE conference on computer vision and pattern recognition*, pages 248–255. Ieee, 2009.

- [15] F. Dörmann, O. Frisk, L. N. Andersen, and C. F. Pedersen. Not all noise is accounted equally: How differentially private learning benefits from large sampling rates. In *2021 IEEE 31st International Workshop on Machine Learning for Signal Processing (MLSP)*, pages 1–6. IEEE, 2021.
- [16] A. Dosovitskiy, L. Beyer, A. Kolesnikov, D. Weissenborn, X. Zhai, T. Unterthiner, M. Dehghani, M. Minderer, G. Heigold, S. Gelly, J. Uszkoreit, and N. Houlsby. An image is worth 16x16 words: Transformers for image recognition at scale. In *International Conference on Learning Representations*, 2021. URL <https://openreview.net/forum?id=YicbFdNTTy>.
- [17] C. Dwork. Differential privacy: A survey of results. In *International Conference on Theory and Applications of Models of Computation*, pages 1–19, 2008.
- [18] C. Dwork and A. Roth. The algorithmic foundations of differential privacy. *Found. Trends Theor. Comput. Sci.*, 9(3-4):211–407, 2014.
- [19] D. Erhan, Y. Bengio, A. Courville, and P. Vincent. Visualizing higher-layer features of a deep network. *University of Montreal*, 1341(3):1, 2009.
- [20] H. Fang, X. Li, C. Fan, and P. Li. Improved convergence of differential private SGD with gradient clipping. In *The Eleventh International Conference on Learning Representations*, 2023. URL <https://openreview.net/forum?id=FRLswckPXQ5>.
- [21] A. Ganesh, M. Haghifam, M. Nasr, S. Oh, T. Steinke, O. Thakkar, A. Thakurta, and L. Wang. Why is public pretraining necessary for private model training? *arXiv preprint arXiv:2302.09483*, 2023.
- [22] S. Gopi, Y. T. Lee, and L. Wutschitz. Numerical composition of differential privacy. In A. Beygelzimer, Y. Dauphin, P. Liang, and J. W. Vaughan, editors, *Advances in Neural Information Processing Systems*, 2021. URL <https://openreview.net/forum?id=GSXEx6iYd0>.
- [23] J. He, X. Li, D. Yu, H. Zhang, J. Kulkarni, Y. T. Lee, A. Backurs, N. Yu, and J. Bian. Exploring the limits of differentially private deep learning with group-wise clipping. In *The Eleventh International Conference on Learning Representations*, 2023. URL <https://openreview.net/forum?id=oze0c1VGPeX>.
- [24] K. He, H. Fan, Y. Wu, S. Xie, and R. Girshick. Momentum contrast for unsupervised visual representation learning. In *Proceedings of the IEEE/CVF conference on computer vision and pattern recognition*, pages 9729–9738, 2020.
- [25] E. Hoffer, T. Ben-Nun, I. Hubara, N. Giladi, T. Hoefler, and D. Soudry. Augment your batch: better training with larger batches, 2019. URL <https://arxiv.org/abs/1901.09335>.
- [26] F. A. Hözl, D. Rueckert, and G. Kaissis. Bridging the gap: Differentially private equivariant deep learning for medical image analysis, 2022.
- [27] F. A. Hözl, D. Rueckert, and G. Kaissis. Equivariant differentially private deep learning, 2023.
- [28] S. Ioffe and C. Szegedy. Batch normalization: Accelerating deep network training by reducing internal covariate shift. In *Proceedings of the 32nd International Conference on Machine Learning, ICML 2015*, volume 37, pages 448–456. JMLR.org, 2015.
- [29] G. Kamath, A. Mouzakis, M. Regehr, V. Singhal, T. Steinke, and J. Ullman. A bias-variance-privacy trilemma for statistical estimation, 2023.
- [30] T. Karras, S. Laine, M. Aittala, J. Hellsten, J. Lehtinen, and T. Aila. Analyzing and improving the image quality of stylegan. In *Proceedings of the IEEE/CVF conference on computer vision and pattern recognition*, pages 8110–8119, 2020.
- [31] H. Kataoka, K. Okayasu, A. Matsumoto, E. Yamagata, R. Yamada, N. Inoue, A. Nakamura, and Y. Satoh. Pre-training without natural images. In *Proceedings of the Asian Conference on Computer Vision*, 2020.
- [32] H. Klause, A. Ziller, D. Rueckert, K. Hammernik, and G. Kaissis. Differentially private training of residual networks with scale normalisation, 2022.

- [33] A. Krizhevsky, G. Hinton, et al. Learning multiple layers of features from tiny images. 2009.
- [34] A. Krizhevsky, I. Sutskever, and G. E. Hinton. Imagenet classification with deep convolutional neural networks. In F. Pereira, C. Burges, L. Bottou, and K. Weinberger, editors, *Advances in Neural Information Processing Systems*, volume 25. Curran Associates, Inc., 2012. URL [https://proceedings.neurips.cc/paper\\_files/paper/2012/file/c399862d3b9d6b76c8436e924a68c45b-Paper.pdf](https://proceedings.neurips.cc/paper_files/paper/2012/file/c399862d3b9d6b76c8436e924a68c45b-Paper.pdf).
- [35] A. Kumar, A. Raghunathan, R. M. Jones, T. Ma, and P. Liang. Fine-tuning can distort pre-trained features and underperform out-of-distribution. In *International Conference on Learning Representations*, 2022. URL <https://openreview.net/forum?id=UYneFzXSJWh>.
- [36] A. B. Lee, D. Mumford, and J. Huang. Occlusion models for natural images: A statistical study of a scale-invariant dead leaves model. *International Journal of Computer Vision*, 41:35–59, 2001.
- [37] T. Li, M. Zaheer, S. Reddi, and V. Smith. Private adaptive optimization with side information. In *Proceedings of the 39th International Conference on Machine Learning*, pages 13086–13105. PMLR, 2022.
- [38] X. Li, D. Liu, T. Hashimoto, H. A. Inan, J. Kulkarni, Y. Lee, and A. G. Thakurta. When does differentially private learning not suffer in high dimensions? In A. H. Oh, A. Agarwal, D. Belgrave, and K. Cho, editors, *Advances in Neural Information Processing Systems*, 2022. URL <https://openreview.net/forum?id=FR--mkQu0dw>.
- [39] X. Li, F. Tramer, P. Liang, and T. Hashimoto. Large language models can be strong differentially private learners. In *International Conference on Learning Representations*, 2022.
- [40] H. Mehta, W. Krichene, A. G. Thakurta, A. Kurakin, and A. Cutkosky. Differentially private image classification from features. *Transactions on Machine Learning Research*, 2023. ISSN 2835-8856. URL <https://openreview.net/forum?id=Cj6pLc1mwT>.
- [41] H. Mehta, A. G. Thakurta, A. Kurakin, and A. Cutkosky. Towards large scale transfer learning for differentially private image classification. *Transactions on Machine Learning Research*, 2023. ISSN 2835-8856. URL <https://openreview.net/forum?id=Uu8WwCFpQv>.
- [42] M. Nasr, S. Mahlouiifar, X. Tang, P. Mittal, and A. Houmansadr. Effectively using public data in privacy preserving machine learning, 2022. <https://openreview.net/pdf?id=5R96mIU85IW>.
- [43] E. Oyallon and S. Mallat. Deep roto-translation scattering for object classification. In *Proceedings of the IEEE Conference on Computer Vision and Pattern Recognition*, pages 2865–2873, 2015.
- [44] A. Panda, X. Tang, V. Schwag, S. Mahlouiifar, and P. Mittal. Dp-raft: A differentially private recipe for accelerated fine-tuning. *arXiv preprint arXiv:2212.04486*, 2022.
- [45] N. Papernot, A. Thakurta, S. Song, S. Chien, and Ú. Erlingsson. Tempered sigmoid activations for deep learning with differential privacy. In *Proceedings of the AAAI Conference on Artificial Intelligence*, volume 35, pages 9312–9321, 2021.
- [46] T. Sander, P. Stock, and A. Sablayrolles. Tan without a burn: Scaling laws of dp-sgd, 2022.
- [47] R. Shokri, M. Stronati, C. Song, and V. Shmatikov. Membership inference attacks against machine learning models. In *2017 IEEE Symposium on Security and Privacy (SP)*, pages 3–18. IEEE, 2017.
- [48] S. Song, K. Chaudhuri, and A. D. Sarwate. Stochastic gradient descent with differentially private updates. In *2013 IEEE Global Conference on Signal and Information Processing*, pages 245–248, 2013. doi: 10.1109/GlobalSIP.2013.6736861.
- [49] F. Tramer and D. Boneh. Differentially private learning needs better features (or much more data). In *International Conference on Learning Representations*, 2021.

- [50] T. Wang and P. Isola. Understanding contrastive representation learning through alignment and uniformity on the hypersphere. In *International Conference on Machine Learning*, pages 9929–9939. PMLR, 2020.
- [51] J. Yang, R. Shi, and B. Ni. Medmnist classification decathlon: A lightweight automl benchmark for medical image analysis. In *IEEE 18th International Symposium on Biomedical Imaging (ISBI)*, pages 191–195, 2021.
- [52] J. Yang, R. Shi, D. Wei, Z. Liu, L. Zhao, B. Ke, H. Pfister, and B. Ni. Medmnist v2-a large-scale lightweight benchmark for 2d and 3d biomedical image classification. *Scientific Data*, 10(1):41, 2023.
- [53] D. Yu, H. Zhang, W. Chen, and T.-Y. Liu. Do not let privacy overbill utility: Gradient embedding perturbation for private learning. *arXiv preprint arXiv:2102.12677*, 2021.
- [54] D. Yu, H. Zhang, W. Chen, J. Yin, and T.-Y. Liu. Large scale private learning via low-rank reparametrization. In *International Conference on Machine Learning*, pages 12208–12218. PMLR, 2021.
- [55] D. Yu, S. Naik, A. Backurs, S. Gopi, H. A. Inan, G. Kamath, J. Kulkarni, Y. T. Lee, A. Manoel, L. Wutschitz, S. Yekhanin, and H. Zhang. Differentially private fine-tuning of language models. In *International Conference on Learning Representations*, 2022.

## A Results on Different Synthetic Data

A number of synthetic datasets have been proposed by prior work. Baradad et al. [4] consider a family of synthetic datasets generated by random processes, and report that the best synthetic datasets in terms of downstream performance is generated by an untrained StyleGAN with a specific initialization, denoted as StyleGAN-Oriented. Based on this prior work, we also use StyleGAN-Oriented as our main synthetic dataset throughout the main body of the paper. We also considered the Shaders dataset proposed in Baradad et al. [5] for our ImageNet experiments. In this subsection we consider different choices of synthetic datasets and find that multiple synthetic datasets can provide good performance. That is, our results and analysis extend beyond StyleGAN-Oriented and can be applied to future proposed synthetic datasets.

We first use the feature extractor checkpoint<sup>3</sup> provided by Baradad et al. [4] pretrained on different synthetic datasets (Please refer Baradad et al. [4] for the full description of these datasets).

Note that Baradad et al. [4] uses a small AlexNet [34] as feature extractor, which includes Batch-Norm [28]. We freeze the feature encoder and only train the last linear model, therefore the feature extractor does not break our differential privacy guarantee. When we use the feature extractor in the main body we use WideResNet without BatchNorm.

Tab. 9 summarizes the results on different synthetic datasets. As in Baradad et al. [4], the best synthetic dataset is StyleGAN-oriented. However, even the worst-performing synthetic dataset (Dead leaves) performs similarly to the best prior work [49; 13].

Table 9: Test accuracy of private linear probing ( $\epsilon = 1$ , training for 100 steps, that is the same as with WRN-16) on a small AlexNet trained on different synthetic images. StyleGAN-Oriented achieves the best performance. Note that all these images are generated without access to real-world images.

	Dead leaves textures	Stat Color+WMM	Untrained StyleGAN			Feature Vis Dead leaves
			Sparse	High freq	Oriented	
Accuracy	59.92	64.59	64.34	64.08	67.79	59.32

## B Ablation Study on Model Architecture

We present DP-RandP on CIFAR10 with experiments with WRN16-4 in the main body and here we also present the WRN40-4 result on CIFAR10 in Tab. 10. The result has a similar trend as De et al. [13], WRN40-4 can achieve better utility with more parameters. For example, at  $\epsilon = 1$ , WRN40-4 has a 0.83% increase compared to WRN16-4. However, training WRN40-4 model takes a longer time. Training a WRN16-4 for 875 steps takes 5.5 hours while the same amount of steps would take 12 hours for WRN40-4. Given the utility improvement is within 2% improvement by changing from WRN16-4 to WRN40-4, we use WRN16-4 to demonstrate the effectiveness of DP-RandP for the main experiments.

Table 10: Ablation study on WRN16-4 and WRN40-4 on CIFAR10.

Method	Model	$\epsilon = 1$	$\epsilon = 2$	$\epsilon = 3$	$\epsilon = 4$	$\epsilon = 6$	$\epsilon = 8$
DP-RandP w/o Phase II	WRN16-4	69.03	75.31	78.44	80.56	82.90	84.45
	WRN40-4	69.45	76.63	79.64	82.20	84.51	85.57
DP-RandP	WRN16-4	72.32	77.25	79.99	81.88	84.01	85.26
	WRN40-4	73.15	77.53	80.93	82.83	85.17	86.12

<sup>3</sup>[https://github.com/mbaradad/learning\\_with\\_noise](https://github.com/mbaradad/learning_with_noise).

## C Hyperparameters

Our experiments are based on the open-source code<sup>4</sup> of Sander et al. [46] and Baradad et al. [4]. We also provide our code. Tab. 11, 12 and 13 summarize the hyperparameters for DP-RandP on CIFAR10, CIFAR100 and DermaMNIST respectively. We use the same total steps and batch size for CIFAR10 by following De et al. [13]. We also use the same hyperparameters for CIFAR100. For DermaMNIST, we use batch size 1024 because Hölzl et al. [26] follow Klause et al. [32] and Klause et al. [32] use batch size 1024. For the noise multiplier  $\sigma$ , given sampling rate and total step size,  $\sigma$  is precomputed according to PRV accounting Gopi et al. [22] with  $\epsilon_{\text{error}} = 0.01$  and rounded up to the precision of 0.1 to ensure that we do not underestimate the privacy loss.

Table 11: Hyperparameters for DP-RandP on CIFAR10. Batch size is 4096 Augmult is 16, SGD optimizer with momentum 0 and no weight decay.

$\epsilon$	1	2	3	4	6	8
Total Steps	875	1125	1593	1687	1843	2468
$\sigma$	9.3	5.6	4.7	3.8	2.9	2.6
Steps in Phase II	96	96	96	96	96	96
LR in Phase II	15	15	15	15	15	15
LR in Phase III	0.4	1	1	1.2	1.2	1.6

Table 12: Hyperparameters for DP-RandP on CIFAR100. Batch size is 4096 and Augmult is 16, SGD optimizer with momentum 0 and no weight decay.

$\epsilon$	3	4	6	8
Total Steps	1593	1687	1843	2468
$\sigma$	4.7	3.8	2.9	2.6
Steps in Phase II	96	96	96	96
LR in Phase II	25	25	25	25
LR in Phase III	1.4	2	2.2	1.8

Table 13: Hyperparameters for DP-RandP on DermaMNIST. Batch size is 1024 and Augmult is 16, SGD optimizer with momentum 0 and no weight decay.

$\epsilon$	1	4	7.42
Total Steps	600	800	800
$\sigma$	13.6	4.6	2.8
Steps in Phase II	48	48	48
LR in Phase II	2	2	2.8
LR in Phase III	0.2	1	1.2

## D Additional Results on DermaMNIST

We follow Hölzl et al. [26] and report the validation accuracy of DermaMNIST in Table 3. Here we also report the test accuracy in Table 14 and we can see DP-RandP outperforms the DP-SGD baseline.

## E Details for Private Linear Probing

For CIFAR10, we follow Baradad et al. [4] and use the alignment and uniformity loss proposed in Wang and Isola [50] to pretrain a feature extractor WRN16-4 on StyleGAN-oriented dataset. Also we follow Baradad et al. [4] and use the third to last layer and the dimension of this layer is 4096. For

<sup>4</sup><https://github.com/facebookresearch/tan> and [https://github.com/mbaradad/learning\\_with\\_noise](https://github.com/mbaradad/learning_with_noise).

Table 14: Test accuracy (%) of DP-RandP on DermaMNIST.

Method	$\epsilon = 1$	$\epsilon = 4$	$\epsilon = 7.42$	$\epsilon = \infty$
DPSGD we evaluated	68.34 <sub>0.28</sub>	71.08 <sub>0.51</sub>	72.58 <sub>0.19</sub>	76.16
DP-RandP	71.19 <sub>0.28</sub>	73.68 <sub>0.24</sub>	75.04 <sub>0.25</sub>	79.70

ImageNet, we use the pretrained ResNet-50 model, which is pretrained on Shaders-21k with MixUp dataset [5] by MoCo [11].

Note that, the right extreme in Figure 6 is slightly higher than 60% at  $\epsilon = 1$ , while the linear probing result in Table 4 is 67.78% at  $\epsilon = 1$ . This is because contrastive learning [50; 10] usually adds additional representation layers for contrastive learning and may keep it for linear probing. As mentioned in earlier, we follow Baradad et al. [4] and use the third to last layer and the dimension of this layer is 4096. While for Figure 6, we keep the exact same architecture as De et al. [13] for a fair comparison where we did not use such embedding layers.

Table 15: Hyperparameters for linear probing CIFAR10 experiments. Other hyperparameters includes full batch size, SGD optimizer with momentum 0.9, 100 steps, no augmentation multiplicity.

$\epsilon$	0.1	0.2	0.5	1	2	3	4	6	8
$\sigma$	339	171	72	38	21	14	11	8	7
LR	0.8	2.2	5.5	10	20	40	40	60	60

Tab. 15 summarize the hyperparameter for DP-RandP without Phase III on CIFAR10 in Section 3.3.

For ImageNet, we use the pretrained ResNet50 checkpoint made available by Baradad et al. [5] using the Shaders dataset and extract features on ImageNet. We apply the formula in Panda et al. [44] to do private linear probing at  $\epsilon = 1, \epsilon = 8$ . Specifically we do full-batch gradient descent with learning rate  $\eta = 0.2$  for  $T = 500$  steps and use Adam. All other implementation details follow Panda et al. [44]: we start from a zero initialization without bias, and do not make use of weight decay or data augmentation or any other regularization methods.

## F Privacy ratio

We give a general privacy budget allocation strategy in Sec. 3.3 and now visualize this strategy on CIFAR10 in Fig. 7, that is consistent with this strategy.

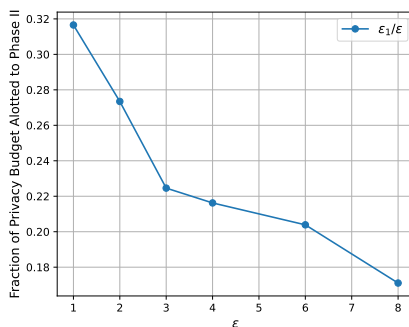


Figure 7: The fraction of total privacy budget allotted to Phase II ( $\epsilon_1/\epsilon$ ) as a function of total privacy budget  $\epsilon$ . As  $\epsilon$  increases, the ratio  $\epsilon_1/\epsilon$  decreases.